OUTER HAIR CELL MECHANICS REFORMULATED WITH ACOUSTIC VARIABLES

JONT B. ALLEN

University of Illinois at Urbana-Champaign, 2061 Beckman Institute for Advanced Science and Technology, 405 North Mathews, Urbana, IL 61801 USA
E-mail: jba@auditorymodels.org

P.F. FAHEY

Dept. of Phys/EE, University of Scranton, Scranton, PA 18510 USA
E-mail: faheyp1@scranton.edu

The electromechanical properties of the Outer Hair Cell (OHC) have been reformulated in terms of acoustic variables. It is anticipated that the acoustic variable formulation will be more useful for incorporating OHC electromechanics into cochlear micromechanics. For guidance on the interdependency of the acoustic and electrical quantities and to aid physical intuition we also present piezoelectric circuit diagram for the OHC.

1 Introduction

The equations for a cylindrical elastic sheathed outer hair cell are [1]

$$\begin{bmatrix} \frac{1}{2}R(\mathcal{P}_t - \mathcal{P}_z) \\ R\mathcal{P}_t \end{bmatrix} = \begin{bmatrix} e_z & e \\ e & e_c \end{bmatrix} \begin{bmatrix} \delta l'_z/l_z \\ \delta R/R \end{bmatrix} = \frac{hE_z}{(1-k\nu^2)} \begin{bmatrix} 1 & k\nu \\ k\nu & k \end{bmatrix} \begin{bmatrix} \delta l'_z/l_z \\ \delta R/R \end{bmatrix}, \quad (1)$$

where $\mathcal{P}_{z,t}$ are the external and internal pressures, l_z is the length of the cell, $\delta l'_z$ represents a change in length, with positive values corresponding to increased length, R and δR represent the radius and change in radius, h is the effective thickness of the cell wall, $e_z = hE_z/\big(1-k\nu^2\big)$, $e_c = hE_c/\big(1-k\nu^2\big)$, $e = \nu hE_c/\big(1-k\nu^2\big)$, where $E_z > 0$ is the axial Young's modulus, ν is a Poisson ratio ($0 \le \nu \le 0.5$) for the axial and circumferential directions with $\nu = \nu_{zc} = \nu_{cz}$, $k \equiv E_c/E_z$ such that $0 < k \le 1$, in terms of either the circumferential or axial Young's modulus E_z and E_c respectively.

If the standard sign convention is followed, $\delta l'$ and δR indicate *increases* in length and radius and the terms involving pressure are signed so that a positive value indicates a tension in the wall of the cell. The physical interpretation of (1) involves the direct stretching in the axial and circumferential directions, and includes the membrane's *Poisson coupling stiffness*, represented by e.

Equation 1 is the two-dimensional Hooke's law for the cell. On the left of the equal sign are the stresses (tensions) on the membrane, expressed in terms of pressure. The force $A_e\mathcal{P}_t$, where $A_e = \pi R^2$, divided by the circumference

$2\pi R$, is the axial tension, acting from within. Since the internal $\mathcal{P}_t$ and external $\mathcal{P}_z$ pressure act on opposite sides of the end-cap, their signs must differ. The stress acting in the circumferential direction may be determined by computing the total force in this direction, $\mathcal{P}_t \times 2R \times l_z$, and dividing by the length over which it is applied $2l_z$.

The matrix of stiffness coefficients ($[e_z, e; e, e_c]$) is symmetric due to membrane reciprocity. The axial and radial stresses and strains are coupled by a "Poisson stiffness" e which accounts for the axial shortening of the membrane as the circumference increases. To visualize this it is helpful to think of the membrane surface laid out flat. When e is nonzero, as the membrane is stretched in one direction, it becomes shorter in the other. This Poisson coupling induces a coupling between the cell's endcap and wall areas, leading to a volume rate change difference which we denote the *Poisson Volume velocity* $\mathcal{V}_p$, elaborated upon in the next section.

2 Results

2.1 Change of sign

We next define a new length $\delta l_z \equiv -\delta l'_z$ by changing the sign of $\delta l'_z$, so that a positive externally applied pressure $\mathcal{P}_z$ gives a positive axial impedance, as required by circuit theory conventions. This transformation leads to

$$\begin{bmatrix} \frac{1}{2}R(\mathcal{P}_z - \mathcal{P}_t) \\ R\mathcal{P}_t \end{bmatrix} = \begin{bmatrix} e_z & -e \\ -e & e_c \end{bmatrix} \begin{bmatrix} \delta l_z/l_z \\ \delta R/R \end{bmatrix}. \tag{2}$$

After this transformation, a shortening of the cell corresponds an *increasing* δl_z.

2.2 Acoustic variables

Equation 2 must be transformed so that the products of the port variables have units of power. One may work in either mechanical variables $[F, \dot{l}]$ or acoustic variables $(\mathcal{P}, \dot{\mathcal{V}})$. Since the cell's turgor pressure $\mathcal{P}_t$ is not conveniently represented as a force, it is best to use acoustical variables, which are natural when working with basilar membrane models.

The *axial volume velocity* $\dot{\mathcal{V}}_z$ is obtained by multiplication of $\dot{l}_z$ by the area of the end cap $A_e \equiv \pi R^2$. Likewise the *radial volume velocity* $\dot{\mathcal{V}}_r$ is obtained by multiplication of $\dot{R}$ by the wall area $A_w \equiv 2\pi R l_z$. These definitions follow from

$$\dot{\mathcal{V}} = A_w \dot{R} + A_e \dot{l}'_z = \dot{\mathcal{V}}_r - \dot{\mathcal{V}}_z \tag{3}$$

where $\dot{\mathcal{V}}$ is the net volume velocity (the time rate of change of the cell volume $\mathcal{V} = A_e l_z = A_w R/2$). A related definition is the *Poisson volume velocity*

$$\dot{\mathcal{V}}_p = \dot{\mathcal{V}}_r + \dot{\mathcal{V}}_z. \tag{4}$$

corresponding to the differential wall and endcap volume velocities resulting from the Poisson coupling stiffness e.

Appling these definitions to (2) results in the cell's acoustic *impedance matrix*

$$\begin{bmatrix} \mathcal{P}_z - \mathcal{P}_t \\ \mathcal{P}_t \end{bmatrix} = \frac{1}{sR\mathcal{V}} \begin{bmatrix} 2e_z & -e \\ -e & \frac{1}{2}e_c \end{bmatrix} \begin{bmatrix} \dot{\mathcal{V}}_z \\ \dot{\mathcal{V}}_r \end{bmatrix}. \tag{5}$$

where $s = i\omega$ is the Laplace frequency. In this acoustic-impedance model, the axial volume velocity is into the cell while the radial volume velocity is out of the cell. For example, when $e = 0$ an increase in the externally applied pressure ($\delta\mathcal{P}_z > 0$) results in an increase in $\mathcal{V}_z$ (i.e., $\delta\mathcal{V}_z > 0$), corresponding to a *shortening* of the cell.

2.3 Physics of the piezoelectric effect.

Warren Mason was the first to show that as a piezoelectric crystal is compressed, the material's bound charge q moves proportionally to the length change δl, namely $q \propto \delta l$ [2]. In the same publication Mason provids a summary of his experimental results in terms of an electrical equivalent circuit. If one assumes that the OHC is piezoelectric, then the OHC model may be implemented as shown in Fig. 1, via two transformers.

The two volume velocities $\dot{\mathcal{V}}_z$ and $\dot{\mathcal{V}}_r$ give rise to the two currents (charge flows) $\dot{q}_z$ and $\dot{q}_r$ which are integrated by the membrane capacitance C_m, resulting in to voltage $v_m(t)$ across the capacitor. Likewise, a change in voltage across the membrane causes a force on the embedded charge, giving rise to two independent strains in the membrane, resulting in a net pressure change (i.e., p_r and p_z). The transformer relations that relate these *efforts* (p, v) and *flows* $(\dot{q}, \dot{\mathcal{V}})$ are

$$\begin{aligned} p_z &= \phi_z v_z, \quad p_r = \phi_r v_r \\ \dot{q}_z &= \phi_z \dot{\mathcal{V}}_z, \quad \dot{q}_r = \phi_r \dot{\mathcal{V}}_r. \end{aligned} \tag{6}$$

Define compliances c_z, c_r and c shown in Fig. 1 as capacitors, as the reciprocal of stiffnesses ($c \equiv 1/k$),

$$\begin{aligned} k_z &= 1/c_z \equiv (2e_z - e)/R\mathcal{V} \\ k_c &= 1/c_r \equiv (e_c/2 - e)/R\mathcal{V} \\ k &= 1/c \equiv -e/R\mathcal{V}. \end{aligned} \tag{7}$$

Having defined the transformers in (6), one may proceed to write down the elastic circuit equations from the circuit diagram

$$\begin{bmatrix} \mathcal{P}_z - \mathcal{P}_t \\ \mathcal{P}_t \\ q_m \end{bmatrix} = \begin{bmatrix} k_z - k & k & \phi_z \\ k & k_c - k & \phi_r \\ -\phi_z & -\phi_r & C_m \end{bmatrix} \begin{bmatrix} \delta\mathcal{V}_z \\ \delta\mathcal{V}_r \\ v_m \end{bmatrix}. \tag{8}$$

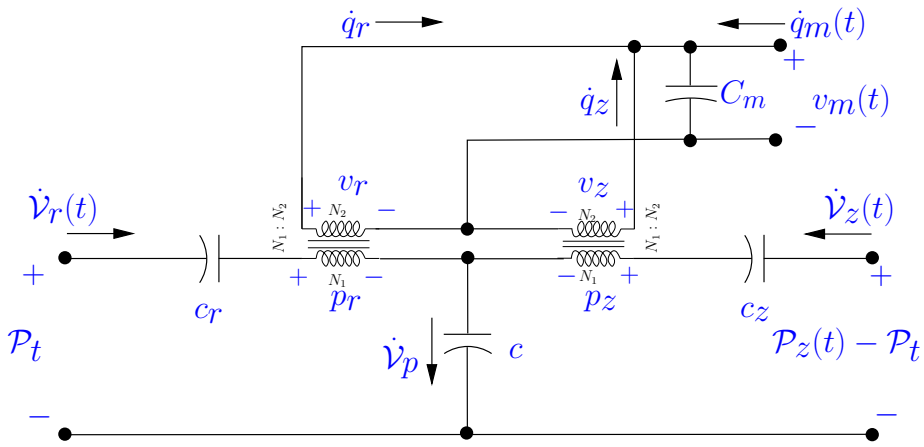

Figure 1. Circuit diagram corresponding to (8).

The first two rows are the loop pressures while the third row is a nodal equation taken at the top of element C_m. This derivation requires the use of (6) and (4). Equation 8 is related to Eqs. (1-3) of [3].

After some algebra the piezoelectric OHC model impedance matrix is

$$\begin{bmatrix} \mathcal{P}_z - \mathcal{P}_t \\ \mathcal{P}_t \\ v_m \end{bmatrix} = \frac{1}{s} \begin{bmatrix} (k_z - k) + \phi_z^2/C_m & k + \phi_z\phi_r/C_m & \phi_z/C_m \\ k + \phi_z\phi_r/C_m & (k_c - k) + \phi_r^2/C_m & \phi_r/C_m \\ \phi_z/C_m & \phi_r/C_m & 1/C_m \end{bmatrix} \begin{bmatrix} \dot{\mathcal{V}}_z \\ \dot{\mathcal{V}}_r \\ \dot{q}_m \end{bmatrix}. \quad (9)$$

Via a term-by-term comparison, the OHC impedance matrix elements z_{ij} are defined by the elements of (9). For example $z_{11} = (k_z - k)/s + \phi_z^2/sC_m$. Note the term $s = i\omega$ must be introduced in the denominator to transform each stiffness into an impedance.

Note that this impedance (stiffness) matrix is positive–symmetric, as required by the electrical circuit representation of Fig. 1. Since every impedance matrix is *positive definite*, all the codeterminants must be positive. The definition of a positive definite matrix, in this context, requires that the total power

$$\dot{\mathcal{V}}_z(\mathcal{P}_z - \mathcal{P}_t) + \dot{\mathcal{V}}_r\mathcal{P}_t + \dot{q}_m v_m \quad (10)$$

is equal to

$$\frac{1}{s}\begin{bmatrix}\dot{\mathcal{V}}_z\\ \dot{\mathcal{V}}_r\\ \dot{q}_m\end{bmatrix}^T\begin{bmatrix}(k_z-k)+\phi_z^2/C_m & k+\phi_z\phi_r/C_m & \phi_z/C_m\\ k+\phi_z\phi_r/C_m & (k_c-k)+\phi_r^2/C_m & \phi_r/C_m\\ \phi_z/C_m & \phi_r/C_m & 1/C_m\end{bmatrix}\begin{bmatrix}\dot{\mathcal{V}}_z\\ \dot{\mathcal{V}}_r\\ \dot{q}_m\end{bmatrix}. \tag{11}$$

Two bulk admittances are relevant to the circuit of Fig. 1, the *unconstrained (i.e., $\mathcal{P}_z = 0$) bulk soma admittance*

$$\mathcal{Y}_\nu \equiv \left.\frac{\dot{\mathcal{V}}}{\mathcal{P}_t}\right|_{\mathcal{P}_z=0} = \frac{\dot{\mathcal{V}}_r - \dot{\mathcal{V}}_z}{\mathcal{P}_t} \tag{12}$$

and the unconstrained membrane *Poisson admittance* due to ν

$$\mathcal{Y}_p \equiv \left.\frac{\dot{\mathcal{V}}_p}{\mathcal{P}_t}\right|_{\mathcal{P}_z=0} = \frac{\dot{\mathcal{V}}_r + \dot{\mathcal{V}}_z}{\mathcal{P}_t}. \tag{13}$$

The physical interpretation of these two bulk admittances are fundamental. The first represents the net volume velocity of the cell per unit pressure. The second represents the proportion of Poisson current $\mathcal{V}_p$ through the capacitor labeled c in Fig. 1. This flow depends only on e (not on e_z or e_c) (see (7)). When $e \to \infty$, $c \to 0$ and $\dot{\mathcal{V}}_p \to 0$. Due to the minus sign in the numerator of (12), $\mathcal{Y}_\nu < \mathcal{Y}_p$, for the case of the unconstrained cell. In the *in vivo* case (i.e., in the constrained cell), $\mathcal{Y}_\nu = 0$. Relations for these admittances in terms of the membrane parameters will be evaluated next.

This concludes the nontrivial transformation from stress-strain membrane variables to acoustic variables.

2.4 Incorporation of Iwasa and Chadwick results

Iwasa and Chadwick (1992) [1] measured the relative axial length change $\delta l_z'/l_z$ and the relative cell radius change $\delta R/R$, as a function of the soma turgor pressure $\mathcal{P}_t$, for isolated OHCs. These measurements were made under the condition of no applied axial force ($\mathcal{P}_z = 0$), and with $v_m = 30$ mv. Note that the cell's volume changes during this measurement, thus $\dot{\mathcal{V}}$ of (3) represents the flow through the pipette.

Iwasa and Chadwick found that the relative length δz and radius δr change are proportional to the turgor pressure, namely

$$\delta z \equiv \delta l_z'/l_z \approx G_z\mathcal{P}_t, \quad \delta r \equiv \delta R/R \approx G_r\mathcal{P}_t. \tag{14}$$

From Fig. 2 of [1], $G_r = 0.13 \times 10^{-3}$ [Pa] and $-G_z \approx 0.069 \times 10^{-3}$. We may rewrite (14) in terms of the acoustic variables (The cell becomes shorter (i.e.,

$\delta\mathcal{V}_z > 0$) with increasing $\mathcal{P}_t$ (i.e., $\delta\mathcal{P}_t > 0$) since $-G_z > 0$.)

$$\dot{\mathcal{V}}_z = -sG_z\mathcal{V}\mathcal{P}_t, \quad \dot{\mathcal{V}}_r = 2sG_r\mathcal{V}\mathcal{P}_t \tag{15}$$

defined in Fig. 1. From (5) with $\mathcal{P}_z = 0$ one may show that

$$\left.\frac{\delta\mathcal{V}_z}{\mathcal{P}_t}\right|_{\mathcal{P}_z=0} = -\mathcal{V}G_z = -k_c/(k_zk_c - k_zk - k_ck) = -R\mathcal{V}\frac{e_c/2 - e}{e_ze_c - e^2} > 0, \tag{16}$$

and

$$\left.\frac{\delta\mathcal{V}_r}{\mathcal{P}_t}\right|_{\mathcal{P}_z=0} = \mathcal{V}G_r = -k_z/(k_zk_c - k_zk - k_ck) = R\mathcal{V}\frac{2e_z - e}{e_ze_c - e^2} > 0. \tag{17}$$

Also

$$\mathcal{Y}_\nu \equiv \left.\frac{\dot{\mathcal{V}}}{\mathcal{P}_t}\right|_{\mathcal{P}_z=0} = (2G_r + G_z)s\mathcal{V} = 0.191 \times 10^{-3}s\mathcal{V}. \tag{18}$$

Given (4) and (15),

$$\dot{\mathcal{V}}_p = (2G_r - G_z)s\mathcal{V}\mathcal{P}_t = 0.329 \times 10^{-3}s\mathcal{V}\mathcal{P}_t, \tag{19}$$

where $\mathcal{P}_t$ is in Pascals, resulting in

$$\mathcal{Y}_p = 0.329 \times 10^{-3}s\mathcal{V}. \tag{20}$$

The product of $\mathcal{V}_p$ and $\mathcal{P}_t$ represents the Poisson coupled elastic energy.

Define $\gamma \equiv G_r/G_z$. From Fig. 1 of [1], $\gamma = -1/0.43 = -2.326$, while from Fig. 2 of [1], $\gamma \equiv G_r/G_z = -1.884$. These two estimates come from different experiments and 6 different cells. An average of these two estimates gives $\gamma = -2.1$. The parameter γ may be interpreted as the reciprocal of the Poisson ratio of some presumed circumferential tubes around the the cell (like barrel hoops). If γ is exactly 2, it would imply that the membrane enveloping the OHC conserves volume. (This might represent fluid and other structures trapped between the cisternae and the cell plasma membrane, for example.) The case of incompressible tubes, $\gamma = -2$, is close to the average value of Iwasa and Chadwick (1992) data. Thus

$$\gamma \equiv \frac{G_r}{G_z} \approx -2 \pm 40\%. \tag{21}$$

From this point on we shall assume that $\gamma = -2$.

From (15)

$$\frac{\dot{\mathcal{V}}_r}{\dot{\mathcal{V}}_z} = -2\gamma \approx 4 \tag{22}$$

For the conditions of the Iwasa and Chadwick (1992) experiment, combining (4) with (21) gives $\dot{\mathcal{V}}_p = 5\dot{\mathcal{V}}_z$. while (3) and (22) give $\dot{\mathcal{V}} = 3\dot{\mathcal{V}}_z$.

2.5 The in vivo cell

At acoustic frequencies, or in the *in vivo* case when the cell is sealed, $\dot{\mathcal{V}} = 0$. From (3) $\dot{\mathcal{V}}_r = \dot{\mathcal{V}}_z$, leading to $\dot{\mathcal{V}}_p = 2\dot{\mathcal{V}}_z$. Assuming no axial load ($\mathcal{P}_z = 0$), and a constant applied voltage ($\dot{q}_m = 0$), the ratio of $\dot{\mathcal{V}}_r$ to $\dot{\mathcal{V}}_z$ may be found from (5)

$$\frac{\dot{\mathcal{V}}_r}{\dot{\mathcal{V}}_z} = -\frac{2e_z - e}{e_c/2 - e} = -\frac{k_z}{k_c}. \tag{23}$$

Combining (22) and (23) gives $k_z \approx -4k_c$, or equivalently $c_z \approx -c_r/4$. Since both $-G_z$ and G_r were found to be greater that zero (see (16) and (17)) it follows that $e_z e_c > e^2$ and that $e > e_c/2$. Thus from (7), $k_c < 0$. From (23), this is the same as saying that as the turgor pressure in increased, the cell becomes fatter and shorter.

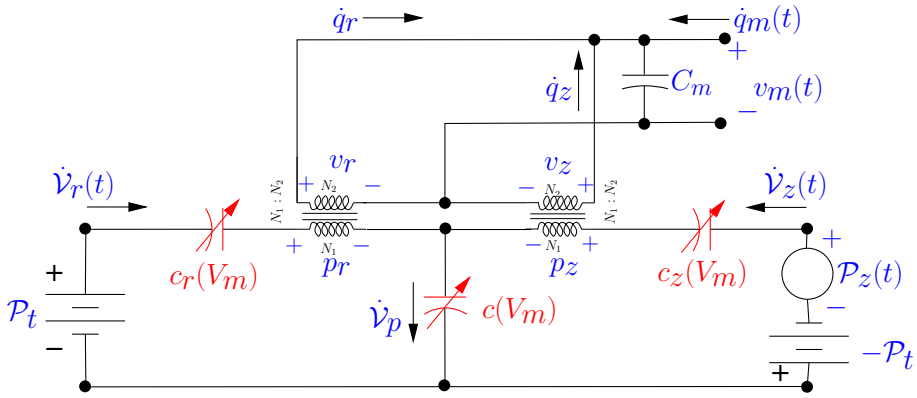

Figure 2. Final circuit diagram with turger pressure as the source. Since the net volume at acoustic frequencies must be zero, $\dot{\mathcal{V}}_z = \dot{\mathcal{V}}_r$, and $\dot{\mathcal{V}}_p = 2\dot{\mathcal{V}}_z$.

Figure 2 shows the configuration of the final curcuit with the membrane compliances shown as voltage dependent, the volume velocity constrained to be

zero, as required at acoustic frequencies, with the turger pressure shown as a battery, the acoustic power source of the cell.

Since $\dot{\mathcal{V}}_z = \dot{\mathcal{V}}_r$, and $\dot{\mathcal{V}}_p = 2\dot{\mathcal{V}}_z$, using the circuit of Fig. 2 one may easily find the turgor pressure and evaluate the axial acoustic impedance of the cell and relate the nonlinear capacitance to the axial loading on the cell. From Eq. 9

$$P_t = \frac{k_c}{k_z + k_c} P_z + \frac{\phi_r k_z - \phi_z k_c}{k_z + k_c} v_m$$

which shows how the turger pressure depends on both the voltage and the axial pressure. This expression may then be substituted back into Eq. 9, and the results may be simplified, for the intact cell constrained to a constant volume, giving

$$\begin{bmatrix} \delta\mathcal{V}_z \\ q_m \end{bmatrix} = \begin{bmatrix} \frac{1}{k_z+k_r} & -\frac{\phi_z+\phi_r}{k_z+k_r} \\ -\frac{\phi_z+\phi_r}{k_z+k_r} & \frac{(\phi_z+\phi_r)^2}{k_z+k_r} + C_m \end{bmatrix} \begin{bmatrix} \mathcal{P}_z \\ v_m \end{bmatrix}. \tag{24}$$

This leads to a very simple result. For the OHC to be nonlinear, either k_z and or k_r must be voltage dependent. Furthermore, this leads to a direct prediction about the voltage dependent nonlinear capacitance, and its relationship to the voltage dependent stiffness and displacement.

3 Conclusion

We have reformulated the OHC constitutive equations in terms of acoustic variables and summarized the electromechanical properties of the OHC with a piezoelectric circuit following Mason's classic model [2]. Future steps will to incorporate OHC NL capacitance along with voltage controlled stiffness results into this scheme. As these data are nonlinear our circuit will necessarily acquire nonlinear voltage–controlled circuit elements. It is our hope that the incorporation of voltage dependent values for $e_z(V_m)$, $e_c(V_m)$ and $e(V_m)$ will be sufficient to represent all of the nonlinear response of the OHC.

We would like to thank Robert Haber for discussions on the form of (1) and on the physical intrepretation of the axial to radial coupling.

References

1. Iwasa, K. and Chadwick, R., 1992. Elasticity and active force generation of cochlear outer hair cells orientation. J. Acoust. Soc. Am 92, 3169–3173.
2. Mason, W.P., 1939. A dynamic measurement of the elastic, electric and piezoelectric constants of rochelle salt. Phys. Rev. 52, 775–789.
3. Spector,A., Brownell, W., and Popel, A., 2003. Effect of outer hair cell piezoelectricity on high-frequency receptor potentials. J. Acoust. Soc. Am. 90, 453–461.